Energy and Spectral Efficiency of Multi-Tier LiFi Networks

Ahmet Burak Ozyurt[1], Rui Bian[2], Harald Haas[2,3], Wasiu O. Popoola[1]
[1]Institute for Digital Communications, School of Engineering, The University of Edinburgh, EH9 3JL, Edinburgh, UK. Email:{a.b.ozyurt, w.popoola}@ed.ac.uk
[2]PureLiFi Ltd, Edinburgh, UK. Email: {rui.bian}@purelifi.com
[3]LiFi Research and Development Center (LRDC), Department of Electronic and Electrical Engineering, University of Strathclyde, Glasgow, G1 1RD, UK. Email: {harald.haas}@strath.ac.uk

***Abstract*—In this paper, multi-tier LiFi networks are studied in terms of energy efficiency (EE) and spectral efficiency (SE), which are crucial metrics for LiFi system design. We derived a closed-form expression of the user association probability for different tiers using stochastic geometry based Poisson Voronoi Tessellation (PVT) LiFi network. The performance metrics of the network, EE and SE, are analyzed in terms of different parameters such as transmit power and Lambertian index. Performance evaluations and numerical results show that multi-tier LiFi networks have an optimum transmit power in which EE is maximized. Besides, increasing the transmit power does not increase SE after passing a threshold point. The resulting trade-off between EE and SE is presented.**

***Keywords*—Multi-tier, energy efficiency, spectral efficiency, visible light communication, LiFi.**

I. INTRODUCTION

The tremendous demand for wireless communication motivates more efficient communication techniques and network topologies. According to [1], mobile networks carried almost 300 times more mobile data in 2021 than in 2011. Energy efficiency, high data rate, huge unlicensed spectrum, and physical layer security all make LiFi, a light-spectrum-based wireless system, a potential technology to address the foregoing challenge [2]. Even though LiFi has the aforementioned advantages compared to conventional RF networks, an even more efficient LiFi network is highly desirable to meet future connectivity demands.

To satisfy the excessive mobile traffic demands and to accommodate the massive number of devices, LiFi network densification via a multi-tier concept has been identified as a key mechanism to tackle the mobile traffic challenges [3]. Having more than one tier in LiFi networks represents realistic scenarios; however, this concept is quite new in the literature and needs better understanding. The different light sources such as the ceiling, floor, and desk lamps can be considered as different tiers in LiFi network.

From the very beginning of wireless communication, two main metrics to measure performance are energy efficiency (EE) and spectral efficiency (SE) [4]. With the enormous increase in communication devices, EE, the transmitted data rate per power consumption, is widely considered in green communication [4]. SE is defined as the transmitted data rate per bandwidth. However, an increase in EE often results in reduced SE. Therefore, a trade-off between SE and EE is always required.

The previous studies on SE and EE in LiFi/visible light communications (VLC) networks can be grouped into two main approaches:

- The first approach is related to the EE and SE in modulation schemes. All of these studies try to differentiate their studies in regard to schemes, such as the direct current (DC) biased optical orthogonal frequency division multiplexing (DCO-OFDM), asymmetrically clipped optical OFDM (ACO-OFDM), OFDM, and spectral and energy efficient OFDM (SEE-OFDM) [5]–[9]. However, obtained results are directly related to physical layer enhancement which is out of the scope of this study.
- The second approach relies on finding the EE and SE on the network level. The study in [10] investigated the trade-off between EE and SE in terms of a new definition of the EE for indoor VLC systems. In [11], an outdoor VLC system is evaluated in regard to EE and SE where an attocell communicate with more than one devices that are capable of harvesting optical energy.

None of the these studies investigated a realistic multi-tier LiFi networks. In the IEEE 802.11bb Task Group on Light Communications, a multiple tiers case in an office environment is proposed which includes two different types of light sources [12]. The authors are not aware of any theoretical or practical work on SE and EE for multi-tier LiFi networks. In our previous works, we investigated cross-tier mobility management in ultra-dense LiFi networks using stochastic geometry [13], [14]. These earlier papers present cell coverage scenario based on the half-angle of the primary and secondary AP light sources. The cross-tier handover

This work is funded by the European Union's Horizon 2020 research and innovation programme under the Marie Skłodowska Curie grant agreement No. 814215 titled ENLIGHT'EM: European Training Network in Low-Energy Visible Light IoT Systems: https://enlightem.eu/.

rate, ping-pong rate, and sojourn time as functions of time to trigger (TTT), AP intensities, and user velocity are presented as closed-form expressions.

This paper investigates SE and EE in multi-tier LiFi networks using stochastic geometry and presents an analytical model. This work is based on a realistic scenario as contained in 'Scenario 2: Office with Secondary Light' in LiFi standards, produced by the IEEE 802.11bb Task Group on Light Communication [12]. The major contributions of this paper are summarized as follows: 1) For the first time in literature, user association probability in multi-tier LiFi network is derived; 2) the impacts of system parameters such as transmit power and Lambertian index on the SE and EE performance are described. This would contribute to the design of more practical LiFi networks; 3) finally, we provide a trade-off point between EE and SE which gives us a working region.

II. SYSTEM MODEL

A. Network Model

In this work, the scenario is based on 'Scenario 2: Office with Secondary Light' which is a part of the LiFi standard as produced by the IEEE 802.11bb Task Group on Light communications [12]. This standard accounts for multiple light sources as access points where the main light source is mounted on the ceiling and a desktop secondary lamp for example. Besides, in our previous work, we investigated the same network model in terms of the cross-tier mobility management in multi-tier LiFi networks using stochastic geometry [13], [14]. Figure 1 and Figure 2 show the exemplary network deployment with two types of light sources; one of them is the main light sources at the ceiling and the other is mounted on the desk to provide task lighting.

The hexagonal or square cell shapes are the most common models for LiFi networks. However, the multiple tiers LiFi networks generally consist of a number of 'statistically random' APs, such as desktop lamps, ceiling luminaries, and even LED screen [3]. The wiring complexity, uncertain lighting requirements, and aesthetic quality make the deployment of LiFi APs completely random [15]. Additionally, even for a uniform cell deployment, some cells may not have users. In that case, the downlink transmission can be switched off, which results in a non-uniform active cell deployment. Thus, deterministic/regular models for the distribution of these APs are impractical and non-realistic [16]. At this point, stochastic geometry helps to model the unpredictability of users in wireless networks [17]. Besides, the analytical framework helps in understanding the effect of various network parameters on the system performance. Thus, this work uses stochastic geometry for the analysis of actual LiFi networks.

In [15], it is observed that hexagonal networks, hard-core point process, or, square networks are lower bounded by the PPP model. Thus, the APs in this paper are distributed randomly from two independent PPPs as a worst case scenario. According to the Slivnyak-Mecke theorem, the statistical characteristics of homogeneous PPP are independent from where the observer's point is located [18]. Thus, it is assumed that users are located at the origin of an xy-plane.

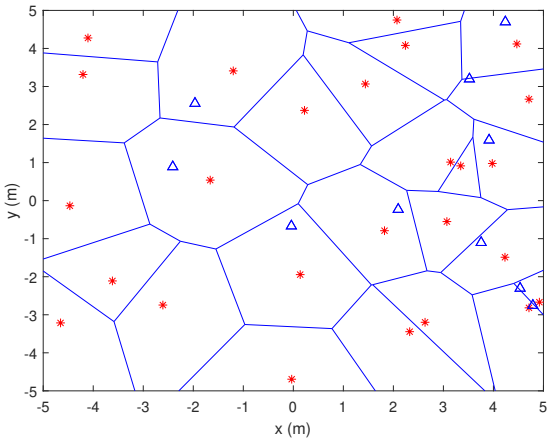

Fig. 1: A concept of multi-tier LiFi network with the primary access points (red stars), the secondary access points (blue triangles), and the cell borders (blue lines).

In multi-tier LiFi networks, primary access points (PAPs) are deployed with high transmit optical power, low spatial density and wider coverage area. On the other hand, secondary access points (SAP), will be a set of other light sources, with lower and smaller coverage area than the PAP. The SAP are very localised and can support higher date rates. Moreover, it is considered that each SAP is covered by a PAP. This system has a central control unit and multiple LiFi transmitters such as in Fig. 1. The frame control, initiating of the scheme, coordination among APs, signal processing, and modulation are all implemented at the central control unit. Besides, the user equipment faces directly upward.

As shown in Fig. 2, a typical PAP is located at the origin, and a SAP is located at position $\mathbf{x_s}(d_1, d_2, d_3)$. For a user located at $(x, y) \in \mathbb{R}^2$ and the PAP height from the ground is h, the distance from user to the PAP (tier $= 1$), and the SAP (tier $= 2$) are given, respectively, by,

$$d_{u,1} = \sqrt{x^2 + y^2 + h^2}, \tag{1}$$

$$d_{u,2} = \sqrt{(x - d_1)^2 + (y - d_2)^2 + (h - d_3)^2}. \tag{2}$$

In addition, $\cos(\varphi_p) = \cos(\psi_p) = \frac{h}{\sqrt{x^2+y^2+h^2}}$ and $\cos(\varphi_s) = \cos(\psi_s) = \frac{h-d_3}{\sqrt{(x-d_1)^2+(y-d_2)^2+(h-d_3)^2}}$ are considered because UE face is assumed to be directed upward.

B. LiFi Channel Model

The optical wireless-based LiFi channel includes two main parts which are line-of-sight (LOS) and non-line-of-sight (NLOS). In this work, only LOS is considered for LiFi network and the effect of NLOS from the walls and human shadowing are ignored because reflected signals are very week and only account for less than 3% of the total received power [15], [19]. Under these assumptions, the LOS channel

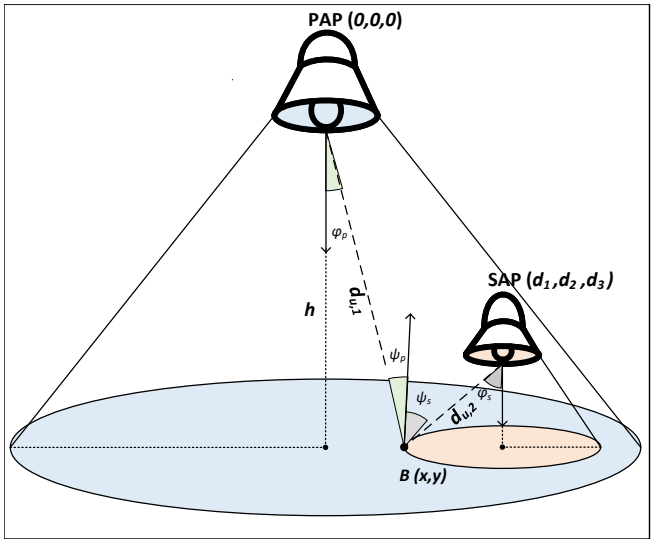

Fig. 2: The multi-tier LiFi network with the primary access point and the secondary access point.

gain $\{\mathrm{H}_{u,j}\}_{j=\{1,\ldots,K\}}$ in tier j for user u is given by [2]:

$$\mathrm{H}_{u,j} = \frac{(m_j+1)A_r}{2\pi d_{u,j}^2}\cos^{m_j}(\varphi_j)T_s g(\psi_j)\cos(\psi_j), \quad (3)$$

where $d_{u,j}$ denotes the distance from the user to an AP in tier j, and the Received Optical Intensity, $\mathrm{ROI_{u,j}} = P_j H_{u,j}$ can be calculated. P_j is the transmit power in the j-th tier, A_r is the receiver effective area, ψ_j is the angle of incidence with respect to the axis normal to the receiver surface, φ_j is the angle of irradiance with respect to the axis normal to the transmitter surface, T_s is the filter transmission factor, ψ_{con} is the field-of-view (FOV), $g(\psi_j)$ is concentrator gain, and m_j is the Lambertian index defined as [2]:

$$m_j = -\frac{\ln(2)}{\ln[\cos(\varphi_{1/2})]}, \quad (4)$$

where $\varphi_{1/2}$ is the semiangle at half illuminance of the transmitter. The gain of the optical concentrator at the receiver is defined by [2]:

$$g(\psi_j) = \begin{cases} n^2/\sin^2(\psi_{con}), & \text{if } 0 \le \psi \le \psi_{con} \\ 0, & \text{if } \psi_{con} \le \psi, \end{cases} \quad (5)$$

where n is the refractive index.

III. User Association Probability in Multi-Tier LiFi Networks

The ROI is the main criteria for assigning a user to a tier. Without of loss of generality, it is assumed that one typical user is served by tier k. Therefore,

$$\mathrm{ROI}_{u,k}(d_{u,k}) > \mathrm{ROI}_{u,j}(d_{u,j}) \quad (6)$$

$$P_k \mathrm{H}_{u,k}(d_{u,k}) > P_j \mathrm{H}_{u,j}(d_{u,j}). \quad (7)$$

When $\mathrm{ROI}_{u,k}(d_{u,k}) > \mathrm{ROI}_{u,j}(d_{u,j})$ for all $j \in \{1\ldots K\}, j \neq k$, a typical user is associated with the k-th tier, i.e. $n = k$. The probability that a typical user is associated with k-th tier, $\mathcal{A}_k$, is derived as follows:

$$\begin{aligned}
\mathcal{A}_k &= \mathbf{P}[n=k] \\
&= \mathbf{E}_{d_k}\Big[\mathbf{P}\big[\mathrm{ROI}_{u,k}(d_{u,k}) > \max_{j,j\neq k}\mathrm{ROI}_{u,j}\big]\Big] \\
&= \mathbf{E}_{d_k}\Big[\prod_{j=1,j\neq k}^{K}\mathbf{P}\big[P_k\mathrm{H}_{u,k}(d_{u,k}) > P_j\mathrm{H}_{u,j}\big]\Big] \\
&\overset{(a)}{=} \mathbf{E}_{d_k}\Big[\prod_{j=1,j\neq k}^{K}\mathbf{P}\Big[d_j > \sqrt{\frac{P_j}{P_k}}\sqrt{\frac{m_j+1}{m_k+1}} \\
&\quad \times \sqrt{\frac{\cos^{m_j+1}(\varphi_j)}{\cos^{m_k+1}(\varphi_k)}}d_k\Big]\Big] \\
&\overset{(b)}{=} \int_0^\infty \Big[\prod_{j=1,j\neq k}^{K}\mathbf{P}\Big[d_j > \widehat{P_j}\widehat{m_j}\sqrt{\frac{\cos^{m_j+1}(\varphi_j)}{\cos^{m_k+1}(\varphi_k)}} \\
&\quad \times d_k\Big] f_{d_k}(l)dl, \quad (8)
\end{aligned}$$

where (a) is given using (3). For clarity of exposition, we define $\widehat{P_j} = \sqrt{\frac{P_j}{P_k}}$ and $\widehat{m_j} = \sqrt{\frac{m_j+1}{m_k+1}}$ in (b). With the help of PPP, the probability, $\mathbf{P}[\text{No AP closer than } l] = e^{-\pi\lambda l^2}$ where the transition length, l, is Rayleigh distributed [20], [21].

$$f_{d_k}(l) = \frac{1-\mathbf{P}[\text{No AP closer than } l]}{dl} = 2\pi\lambda_k l e^{-\pi\lambda_k l^2} \quad (9)$$

Thus,

$$\begin{aligned}
&\prod_{j=1,j\neq k}^{K}\mathbf{P}\Big[d_j > \widehat{P_j}\widehat{m_j}\sqrt{\frac{\cos^{m_j+1}(\varphi_j)}{\cos^{m_k+1}(\varphi_k)}}d_k\Big] \\
&= \prod_{j=1,j\neq k}^{K}\mathbf{P}[\text{No AP closer than } d_j > \widehat{P_j}\widehat{m_j} \\
&\quad \times \sqrt{\frac{\cos^{m_j+1}(\varphi_j)}{\cos^{m_k+1}(\varphi_k)}}d_k \text{ in the } j\text{-th tier}] \\
&= \prod_{j=1,j\neq k}^{K} e^{-\pi\lambda_j\left[\widehat{P_j}\widehat{m_j}\sqrt{\frac{\cos^{m_j+1}(\varphi_j)}{\cos^{m_k+1}(\varphi_k)}}d_k\right]^2} \quad (10)
\end{aligned}$$

Combining (8), (9), and (10), we obtain:

$$\begin{aligned}
\mathcal{A}_k =& 2\pi\lambda_k\int_0^\infty l\exp\Big\{-\pi\sum_{j=1,j\neq k}^{K}\lambda_j\Big[\widehat{P_j}\widehat{m_j} \\
&\times\sqrt{\frac{\cos^{m_j+1}(\varphi_j)}{\cos^{m_k+1}(\varphi_k)}}d_k\Big]^2 - \pi\lambda_k l^2\Big\}dl. \quad (11)
\end{aligned}$$

For different APs in the same tier, $j = k$, $\widehat{P_j} = 1$ and $\widehat{m_j} = 1$. Thus, we obtain the user association probability in

multi-tier LiFi networks as:

$$\mathcal{A}_k = 2\pi\lambda_k \int_0^\infty l \exp\Bigg\{ -\pi \sum_{j=1}^{K} \lambda_j \Bigg[\widehat{P_j}\widehat{m_j} \times \sqrt{\frac{\cos^{m_j+1}(\varphi_j)}{\cos^{m_k+1}(\varphi_k)}} d_k\Bigg]^2\Bigg\} dl. \quad (12)$$

Also, change of variables $l^2 = t$, can be employed. Thus, the defined function in (12), can be simplified to:

$$\mathcal{A}_k = \frac{\lambda_k P_k m_k \cos^{m_k+1}(\varphi_k)}{\sum_{j=1}^{K} \lambda_j P_j m_j \cos^{m_j+1}(\varphi_j)}. \quad (13)$$

The derived closed-form expression shows the relationship between the probability of user associated with k-th tier and other parameters such as AP density, transmit power, Lambertian index. To obtain the numerical result of user association probability, the coverage boundary of the secondary cell should be calculated because of $\cos^{m_k+1}(\varphi_k)$ and $\cos^{m_j+1}(\varphi_j)$ expressions in (13). More details about secondary cell coverage radius is given in [13].

IV. Energy and Spectral Efficiency of Multi-Tier LiFi Networks

With the help of the stochastic geometry, we can model and analyze the behaviour of a UE and APs in the system model. Then the obtained results will be generalized to the whole network. It is important to note that as the same frequency and light spectrum is reused in each LiFi AP in the same tier, therefore, the signal received from unintended LiFi AP in the same tier is perceived as interference. To this end, the Signal-to-Interference-plus-Noise Ratio (SINR) in the LiFi for the user u connected to the LiFi AP k is given by [22]:

$$\text{SINR}_{u,k} = \frac{(P_{u,k}\text{H}_{u,k}\mathcal{R})^2}{\sum_{j=1,j\neq k}^{K}(P_{u,j}\text{H}_{u,j}\mathcal{R})^2 + N_{\text{LiFi}}B_{\text{LiFi}}} \quad (14)$$

where $\mathcal{R}$ is PDs responsivity, N_{LiFi} is the single sided power spectral density (PSD) of LiFi noise, B_{LiFi} is the single-sided bandwidth of the LiFi system.

In this work, one of the most widely used optical modulation schemes, DCO-OFDM, is preferred. In DCO-OFDM, a direct current bias is added to generate a unipolar signal. In addition, to realise real-valued OFDM waveform, Hermitian symmetry is imposed on the subcarriers of the OFDM frames. Thus, the capacity estimation can be conducted using the Shannon-Hartley theorem to calculate the efficiency of the LiFi network [23]. The ergodic capacity is the average rate between the LiFi AP k and user u is calculated in [24], [23] as follow:

$$\mathcal{C}_k = \mathbf{E}[\log_2(1 + \text{SINR}_{u,k})]. \quad (15)$$

Network architecture is designed based on trade-offs between SE and EE. However, it should be emphasized that there is no clear advantage of one metric over the other. Both of them are equally important, and considered when a network is designed.

In this part, EE and SE, which are the maximum total number of bits that the network can deliver per Joule and the sum of the maximum average data rates, are evaluated in regard to multi-tier LiFi networks. Along the lines of [7], the SE can be formulated as

$$\eta_{SE} = \sum_{k=1}^{K} \frac{\mathcal{A}_k \mathcal{C}_k}{B_{\text{LiFi}}}, \quad (16)$$

where $\mathcal{A}_k$ and $\mathcal{C}_k$ are user association probability and the ergodic capacity of each user in the k-th tier, respectively. Additionally, the EE of the system can be determined as [25]:

$$\eta_{EE} = \sum_{k=1}^{K} \frac{\mathcal{A}_k \mathcal{C}_k}{P_{\text{total}}}. \quad (17)$$

According to [26], it is possible to model power consumption of LiFi access point like $\text{P}_{\text{total}} = \sum_{j=1}^{K} \alpha_j P_j + \beta_j$ where P_j denotes the electrical power due to data transmission, β_j is non-transmission related power consumption, which corresponds to the hardware power consumption such as electronic circuits, processors, and backup batteries [27]. Also, internal losses like the feeders cause the difference between consumed and radiated power. Thus, α_j represents this difference as a scaling factor.

V. Performance Evaluation and Numerical Results

In this section, we discuss the performance results of the multi-tier LiFi networks. Unless otherwise stated, the system has two tiers, the relationship between transmit powers is set as $P_1 = 5P_2 = 10$ W and the tier densities $\lambda_1 = 0.3\lambda_2 = 1$ [node/m^2] for this illustration environment. To show the effect of different Lambertian indices on the performance, the semiangle at half illuminance of the transmitters are selected as in Table I. Also, simulation parameters used throughout the paper are shown in Table II.

Fig. 3 shows the relationship between user association probability for the primary tier, $\mathcal{A}_1$, and transmit powers proportion of different tiers, P_1/P_2. Due to two tiers system, the user assocaition probability for the secondary tier is $\mathcal{A}_2 = (1-\mathcal{A}_1)$. With the increase in the primary tier transmit power compared to the secondary tier, the user association probability of the primary tier also increases. This is because the ROI of the primary tier gets higher as transmit power of the primary tier increases, which means that users are attached more easily to the primary tier. On the other hand, the greater Lambertian index of the secondary tier is a reason for the higher user association probability for the primary tier. It should be highlighted that the greater values of the

Table I: Lambertian indices of the access points

	Semiangle at Half Illuminance	
Lambertian Indices	Primary Acces Point	Secondary Access Point
$m_p = m_s$	60°	60°
$m_p > m_s$	30°	60°
$m_p < m_s$	60°	30°

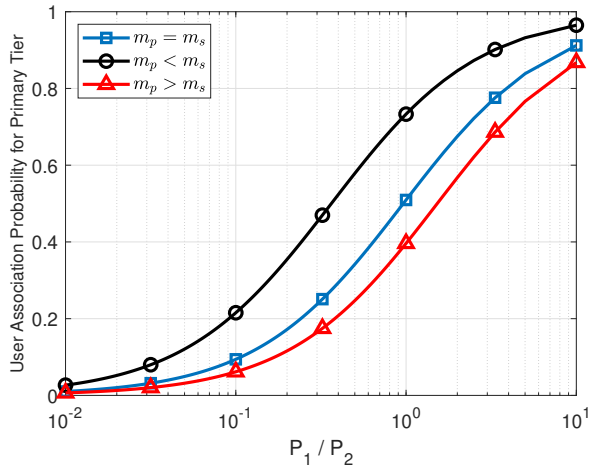

Fig. 3: User association probability of primary tier for varying proportion of transmitter powers in a LiFi network.

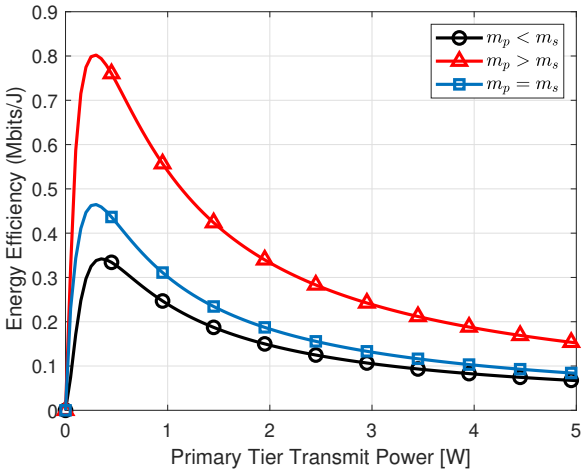

Fig. 5: Energy efficiency of a multi-tier LiFi network for different Lambertian indices and transmit powers.

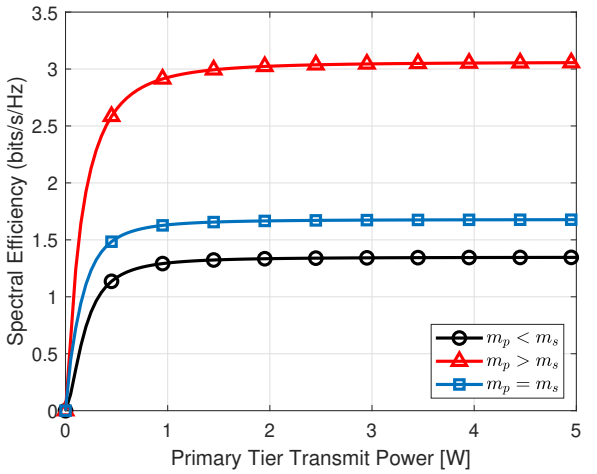

Fig. 4: Spectral efficiency of a multi-tier LiFi network for different Lambertian indices and transmit powers.

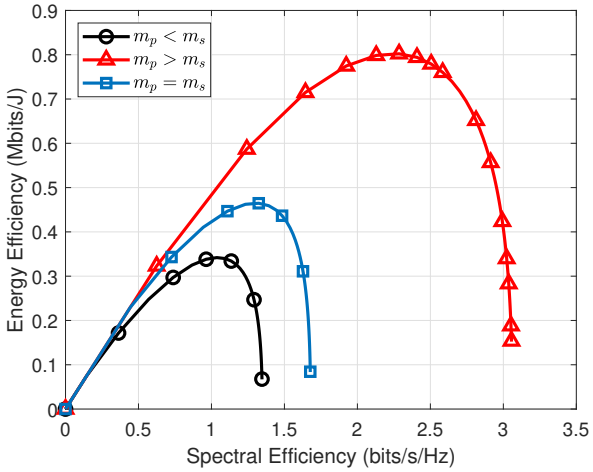

Fig. 6: Trade-off between energy and spectral efficiency of a multi-tier LiFi network in terms of different Lambertian indices and varying primary tier transmit power.

Lambertian index have smaller values of the semi-angle at half illuminance of the transmitter such as in Table I. As expected, a larger semiangle at half illuminance provides a wider coverage area for the primary tier, $m_p < m_s$, when compared with $m_p > m_s$. Because the coverage area of the primary tier for the case $m_p < m_s$ is wider than other cases, the user association probability for the primary tier is also higher than others.

Furthermore, Fig. 4 shows that SE grows rapidly with the transmit power, however, it almost saturates after some point. In this case the larger Lambertian index is the advantage for SE and EE due to providing a smaller coverage area. Network densification with small coverage areas is considered to improve the SE and EE of next-generation mobile networks. Thus, the greater value of the Lambertian index for the primary tier has a higher value of SE and EE. Besides, Fig. 5 shows that an increase in the transmit power cannot help to improve EE after a threshold.

As a significant result of this paper, Fig. 6 demonstrates the trade-off between EE and SE, showing that improving SE does not always accompany an EE enhancement. In fact, the concavity of the curves proves the existence of an optimum point in the trade-off between EE and SE. Besides, it can be observed that this happens approximately when SE approaches its saturation region.

The obtained results are valid and consistent with the previous network level works, especially in terms of the SE saturating after some point, an increase in the transmit power does not improve the EE after a threshold, and the trade-off between SE and EE [5], [6], [24]. It is also to be highlighted that this paper is a preliminary work on EE and the SE of

Table II: Simulation Parameters

Parameter	Value
Photodiode Responsivity (R)	0.53 A/W
Room Dimensions	10 x 10 x 3 m
UE Height	0.75 m
SAP Height	1.2 m
PAP Height	3 m
Bandwidth per LiFi AP (B_{LiFi})	40 MHz
PSD of LiFi Noise (N_{LiFi})	$10^{-21} A^2/Hz$
Receiver Effective Area (A_r)	1 cm^2
Field of View (FOV) of PD (ψ_{con})	60°
Gain of Optical Filter ($g(\psi_j)$)	1
Filter Transmission (T_s)	1
Scaling Factors (α_1, α_2)	{3, 2}
Non-transmission Related Power Consumption (β_1, β_2)	{10, 5 } W

multi-tier LiFi networks. Thus, a dynamic control approach or other system models will be the subject of further studies. The result of this work provides better system-level design insight for the energy and spectral efficient LiFi networks and it contributes to shaping more realistic scenarios.

VI. CONCLUSION

In this work, EE and SE are analyzed as key performance metrics for the multi-tier LiFi networks. Based on received optical intensity, the closed-form expression for the user association for different tiers is derived with the help of stochastic geometry. From the closed-form expressions, it is clear that AP density, transmit power, and Lambertian index are crucial parts of the multi-tier LiFi networks. In addition, numerical evaluations showed that energy and spectral efficiency has an optimum point for the trade-off. The results are valuable in practical LiFi design and development.

REFERENCES

[1] F. Jejdling *et al.*, "Ericsson mobility report," *Ericsson, Stockholm, Sweden, Tech. Rep.*, Nov. 2021.

[2] Z. Ghassemlooy, W. Popoola, and S. Rajbhandari, *Optical wireless communications: system and channel modelling with Matlab®*. CRC press, 2019.

[3] H. Haas, L. Yin, Y. Wang, and C. Chen, "What is lifi?" *Journal of Lightwave Technology*, vol. 34, no. 6, pp. 1533–1544, 2016.

[4] A. B. Ozyurt, M. Basaran, M. Ardanuc, L. Durak-Ata, and H. Yanikomeroglu, "Intracell frequency band exiling for green wireless networks: Implementation, performance metrics, and use cases," *IEEE Vehicular Technology Magazine*, vol. 16, no. 2, pp. 31–39, 2021.

[5] Y. Hei, X. Liu, W. Li, S. Wang, and M. Huo, "Energy- and spectral- efficiency tradeoff in nonlinear ofdm system of visible light communications," *Journal of Lightwave Technology*, pp. 1–1, 2021.

[6] Y. Hei, Y. Kou, G. Shi, W. Li, and H. Gu, "Energy-spectral efficiency tradeoff in dco-ofdm visible light communication system," *IEEE Transactions on Vehicular Technology*, vol. 68, no. 10, pp. 9872–9882, 2019.

[7] Y. Sun, F. Yang, and L. Cheng, "An overview of ofdm-based visible light communication systems from the perspective of energy efficiency versus spectral efficiency," *IEEE Access*, vol. 6, pp. 60 824–60 833, 2018.

[8] H. Elgala and T. D. C. Little, "See-ofdm: Spectral and energy efficient ofdm for optical im/dd systems," in *2014 IEEE 25th Annual International Symposium on Personal, Indoor, and Mobile Radio Communication (PIMRC)*, 2014, pp. 851–855.

[9] S. Ma, R. Yang, X. Deng, X. Ling, X. Zhang, F. Zhou, S. Li, and D. W. K. Ng, "Spectral and energy efficiency of aco-ofdm in visible light communication systems," *IEEE Transactions on Wireless Communications*, pp. 1–1, 2021.

[10] E. Li, W. Zhang, J. Sun, C.-X. Wang, and X. Ge, "Energy-spectral efficiency tradeoff of visible light communication systems," in *2016 IEEE/CIC International Conference on Communications in China (ICCC)*, 2016, pp. 1–5.

[11] A. M. Abdelhady, O. Amin, A. Chaaban, B. Shihada, and M.-S. Alouini, "Spectral-efficiency—illumination pareto front for energy harvesting enabled vlc systems," *IEEE Transactions on Communications*, vol. 67, no. 12, pp. 8557–8572, 2019.

[12] M. Uysal, F. Miramirkhani, T. Baykas, and K. Qaraqe, "IEEE 802.11 bb reference channel models for indoor environments," Tech. Rep., 2018.

[13] A. B. Ozyurt and W. O. Popoola, "Mobility management in multi-tier LiFi networks," *IEEE/OSA Journal of Optical Communications and Networking*, vol. 13, no. 9, pp. 204–213, 2021.

[14] A. B. Ozyurt, I. Tinnirello, and W. O. Popoola, "Modelling of multi-tier handover in lifi networks," in *GLOBECOM 2021 - 2021 IEEE Global Communications Conference*, 2021, pp. 1–6.

[15] C. Chen, D. A. Basnayaka, and H. Haas, "Downlink performance of optical attocell networks," *Journal of Lightwave Technology*, vol. 34, no. 1, pp. 137–156, 2016.

[16] A. B. Ozyurt and W. O. Popoola, "Comp-jt scheme for d2d communication in industrial lifi networks," *IEEE Access*, vol. 10, pp. 70 760–70 768, 2022.

[17] M. Haenggi, *Stochastic geometry for wireless networks*. Cambridge University Press, 2012.

[18] D. Stoyan, W. S. Kendall, S. N. Chiu, and J. Mecke, *Stochastic geometry and its applications*. John Wiley & Sons, 2013.

[19] A. B. Ozyurt and W. O. Popoola, "Lifi-based d2d communication in industrial iot," *IEEE Systems Journal*, pp. 1–8, 2022.

[20] H.-S. Jo, Y. J. Sang, P. Xia, and J. G. Andrews, "Heterogeneous cellular networks with flexible cell association: A comprehensive downlink sinr analysis," *IEEE Transactions on Wireless Communications*, vol. 11, no. 10, pp. 3484–3495, 2012.

[21] X. Xu, C. Yuan, W. Chen, X. Tao, and Y. Sun, "Adaptive cell zooming and sleeping for green heterogeneous ultradense networks," *IEEE Transactions on Vehicular Technology*, vol. 67, no. 2, pp. 1612–1621, 2018.

[22] R. Ahmad, M. D. Soltani, M. Safari, and A. Srivastava, "Load balancing of hybrid lifi wifi networks using reinforcement learning," in *2020 IEEE 31st Annual International Symposium on Personal, Indoor and Mobile Radio Communications*, 2020, pp. 1–6.

[23] T. Z. Gutema, H. Haas, and W. O. Popoola, "Bias point optimisation in lifi for capacity enhancement," *Journal of Lightwave Technology*, pp. 1–1, 2021.

[24] A. R. Khamesi and M. Zorzi, "Energy and area spectral efficiency of cell zooming in random cellular networks," in *Global Communications Conference (GLOBECOM), 2016 IEEE*. IEEE, 2016, pp. 1–6.

[25] M. D. Soltani, M. A. Arfaoui, I. Tavakkolnia, A. Ghrayeb, M. Safari, C. M. Assi, M. O. Hasna, and H. Haas, "Bidirectional optical spatial modulation for mobile users: Toward a practical design for lifi systems," *IEEE Journal on Selected Areas in Communications*, vol. 37, no. 9, pp. 2069–2086, 2019.

[26] A. Khreishah, S. Shao, A. Gharaibeh, M. Ayyash, H. Elgala, and N. Ansari, "A hybrid rf-vlc system for energy efficient wireless access," *IEEE Transactions on Green Communications and Networking*, vol. 2, no. 4, pp. 932–944, 2018.

[27] A. Khreishah, S. Shao, and A. Gharaibeh, "A hybrid rf-vlc system for energy efficient wireless access," *IEEE Transactions on Green Communications and Networking*, vol. 2, no. 4, pp. 932–944, 2018.